Advances in IT and Electrical Engineering

vol. 30, 2024, 5-11
https://doi.org/10.7862/re.2023.x

THE FACULTY OF ELECTRICAL AND COMPUTER ENGINEERING
RZESZOW UNIVERSITY OF TECHNOLOGY

Original Research/Review

Modeling of the textronic structure using the Iterative Fundamental Solutions Method

Mariusz Mączka [2]*, Stanisław Pawłowski [1], Jolanta Plewako [3],

[1] Department of Electrodynamics and Electrical Machine Systems, Faculty of Electrical and Computer Engineering, Rzeszow University of Technology, 35-959 Rzeszow, Poland; spawlo@prz.edu.pl.
[2] Department of Electronics Fundamentals, Faculty of Electrical and Computer Engineering, Rzeszow University of Technology, 35-959 Rzeszow, Poland; mmaczka@prz.edu.pl.
[3] Department of Power Electronics and Power Engineering, Faculty of Electrical and Computer Engineering, Rzeszow University of Technology; 35-959 Rzeszow, Poland, jplewako@prz.edu.pl.

*Corresponding author. mmaczka@prz.edu.pl

Received: 30 June 2023 / Accepted: 06 February 2024 / Published online: 13 February 2024

Abstract

The paper describes an approach to modelling the conductance of a textronic structure based on the iterative fundamental solutions method. The analysis of the current density distribution in a thin conductive layer containing roughness resulting from the applied manufacturing technology is aimed at estimating its impact on the total current and the conductivity of the conductive path. The simulations showed that the current density distribution in a conductive path depends on the nature of its surface, and increasing its roughness reduces its conductance. The proposed solution makes it possible to define a structure model in three geometrical dimensions, and its numerical implementation in the form of the proposed method ensures efficiency and computational accuracy.

Keywords: Fundamental Solutions Method, Textronic Structure

1. Introduction

Textronic structures are a complex class of materials that combine the features of electronic devices and textile structures. Due to their unique properties, such as high mechanical strength, flexibility, and electrical conductivity, these materials are widely used in areas such as electronics, medicine, automation, and textiles [1].

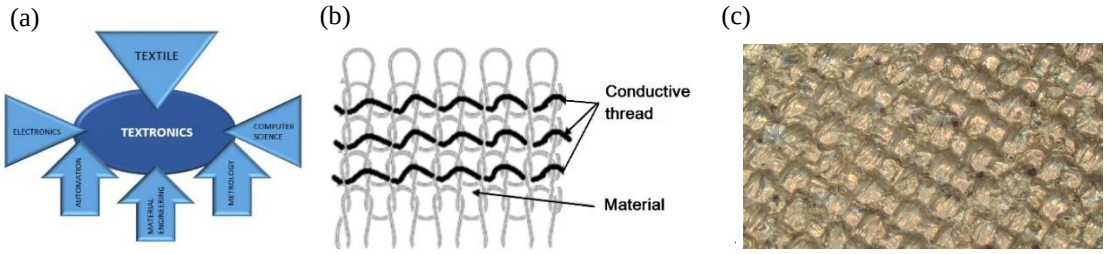

Fig. 1. The textronics area (a) [4] and typical realizations of textronic structures: conductive threads intertwined between the fibers (b) [4], conductive surfaces sputtered onto the textile material (c)

Textronic products are currently used most frequently in uniformed and rescue services and as everyday items [2]. From the textile technology side, textronic systems require the use of materials such

as fibers, threads, electrically conductive fabrics, piezoelectric fabrics, magnetic fibers, optical fibers and textiles with shape memory as well as electroactive polymers. As electronic systems, these structures should show adequate accuracy and repeatability of response to control signals as well as resistance to external factors such as humidity or temperature. The implementation of such structures can be achieved by interlacing thin conductive threads between the fibers of the textile material [3] or using the physical vapour deposition (PVD) method [4]. Based on textronic structures, sensors and wearable electronic devices are built in the form of clothing, jewelry, watches, wristbands, glasses and others. Thanks to them, various physiological, environmental or behavioral parameters of the user, such as heart rate, blood pressure, body temperature, blood, glucose level, body position, movements, physical activity or location, can be monitored in real time [5-8]. The basis for the continuous development of the above technologies is the ability to implement new solutions using computer models that optimize project costs. In this area, numerical models dedicated to structures composed of thin conductive threads are known [9-11], but there is a still deficit of models intended for layered structures made using the PVD method. Existing models [12-13] assume infinitely thin conductive layers, limiting the model geometry to 2 dimensions. This article is the result of work aimed at expanding the possibilities of simulation in the above-mentioned area

The aim of this work is to develop a three-dimensional textronic structure model (3D TSM) realised by using the PVD method. Analysis of the distribution of current density in a thin conductive layer that contains narrowing resulting from the gravitational deposition of conductive particles on the fabric aims to estimate its impact on the total current and conductance of the conductive path.

2. Formulation of the problem

A model of a conductive layer deposited on a textile substrate is considered, which is illustrated in Fig. 2. The analysed area Ω is limited by six surfaces marked as S_1, …, S_6. Surfaces S_1, …, S_4 are flat, and the surfaces S_5 and S_6 spaced d apart have periodically distributed ridges and depressions. Its shape and arrangement can generally be different and depend on the type of textile fabric weave that is modelled. In this work, it was assumed to model them using the sine functions with a given amplitudes A_1 and A_2 for S_5 and S_6 surfaces respectively. These functions are mutually perpendicular and run in directions parallel to the surface of the fabric.

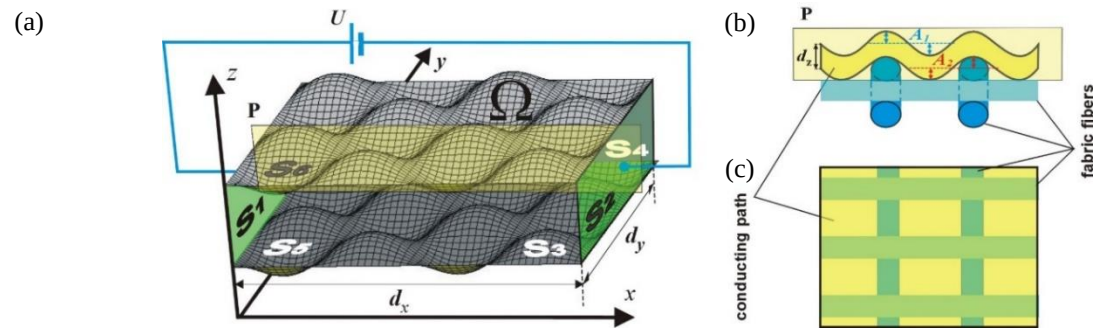

Fig. 2. Simplified concept of the 3D Textronic Structure Model (3D TSM): boundary surfaces and voltage polarization system (a); view of the model in a cross-section with plane P (b) and top view of the model (c)

The mathematical description of the area modelling the conductive layer on the textile substrate is presented by the relations:

$$\Omega:\begin{cases} 0 \le x \le d_x \\ 0 \le y \le d_y \\ A_2(1+\sin k_x x \sin k_y y) \le z \le A_1(1+\sin k_x x \sin k_y y) + d_z \end{cases} \tag{1}$$

It is assumed that the area Ω is filled with a homogeneous, isotropic and linear conductor (γ = const), in which there are no unbalanced electric charges (ρ = 0), its surroundings are an ideal dielectric (γ_0 = 0) and that there is a constant voltage U between the surfaces S_1 and S_2 (see Fig. 2).

For the assumptions presented above, the problem of calculating the current flow field boils down to searching for the distribution of electric potential defined as:

$$\mathbf{E} = -\operatorname{grad}\varphi \tag{2}$$

where $\vec{E}$ is the electric field strength. The potential φ meets the Laplace equation:

$$\Delta\varphi = 0 \tag{3}$$

and mixed boundary conditions:

$$\varphi = U \text{ on the surface } S_1 \tag{4}$$

$$\varphi = 0 \text{ on the surface } S_2 \tag{5}$$

$$\frac{\partial\varphi}{\partial n} = 0 \text{ on the surface } S_i,\ i = 3, 4, 5, 6 \tag{6}$$

After solving the problem formulated above, the current density distribution sought is determined on the basis of (2) and the local Ohm's law:

$$\mathbf{J} = \gamma\,\mathbf{E} \tag{7}$$

and the current from the dependence:

$$I = \iint_S \mathbf{J}\cdot \mathrm{d}\,s\,, \tag{8}$$

where s can be any section of the area Ω connecting the surfaces S_3 and S_4 (e.g. for x = const)

3. Solution of the problem

In order to solve the problem described by formulas (3) - (6), the fundamental solutions method (FSM) was applied [5]. In the next iteration steps, successive approximations of the sought potential function are calculated according to the formula:

$$\tilde{\varphi}_k(\mathbf{r}) = \tilde{\varphi}_{k-1}(\mathbf{r}) + \sum_{n=1}^{L_\mathrm{f}} q_{k,n} F_{k,n}(\mathbf{r}) \tag{9}$$

where: k – iteration step number,

$\mathbf{r} = (x, y, z)$ – any point within the Ω area,

$q_{k,n}$ – approximation sum coefficients calculated on the basis of boundary conditions,

$F_{k,n}(\mathbf{r}) = \dfrac{1}{|\mathbf{r} - \mathbf{r}_{k,n}|}$ – fundamental solution of the Laplace equation,

$\mathbf{r}_{k,n}$ – fixed points lying outside the Ω area (singular points of the function $F_{k,n}$),

L_f – the number of fundamental solutions considered in a single iteration step.

The function $\tilde{\varphi}_0(\mathbf{r})$ was assumed (primary field):

$$\tilde{\varphi}_0(\mathbf{r}) = U\left(1 - \frac{x}{d_x}\right) \tag{10}$$

This function satisfies equation (3) and boundary conditions (4) - (6) on the surfaces: S_1, S_2, S_3, S_4, which significantly accelerates the convergence of calculations. It should also be noted that regardless of the value of the coefficients $q_{k,n}$ each function described by the formula (9) satisfies equation (3) exactly, and the selection of points outside the Ω area $\mathbf{r}_{k,n}$ guarantees its finiteness in this area.

The values of the coefficients $q_{k,n}$ are determined in such a way as to obtain the best possible improvement of the fulfillment of the boundary conditions by the function $\tilde{\varphi}_k(\mathbf{r})$ in a given iteration step in relation to the iteration calculated in the previous step. For this purpose, a measure of the accuracy of meeting the boundary conditions by the function $\tilde{\varphi}_k(\mathbf{r})$ should be defined. On individual boundary surfaces of the area, functions of local, relative edge errors of the solution are:

$$\varepsilon_{1,k}(\mathbf{r}) = \frac{1}{U}\left(U - \tilde{\varphi}_k(\mathbf{r})\right), \quad \mathbf{r} \in \mathrm{S}_1 \tag{11}$$

$$\varepsilon_{2,k}(\mathbf{r}) = \frac{1}{U}\tilde{\varphi}_k(\mathbf{r}), \quad \mathbf{r} \in \mathrm{S}_2 \tag{12}$$

$$\varepsilon_{i,k}(\mathbf{r}) = \frac{1}{E_0}\frac{\partial\tilde{\varphi}_k}{\partial n}, \quad \mathbf{r} \in \mathrm{S}_i, \quad i = 3,\ldots,6 \tag{13}$$

where: $E_0 = \dfrac{U}{d_x}$ is the primary electric field strength (see eq. (10), (2)), and *the boundary error functional*:

$$\delta_k = \sqrt{\sum_{i=1}^{6}\frac{1}{S_i}\iint_{\mathrm{S}_i}\varepsilon_{i,k}^2(\mathbf{r})\,\mathrm{d}s} \tag{14}$$

which is a measure, in the sense of the mean square norm, of jointly meeting the boundary conditions (4) - (6) by solution (9). Postulating the minimization of this functional with respect to the set of parameters $q_{k,n}$

$$\frac{\partial\delta_k}{\partial q_{k,m}} = 0, \quad m = 1,\ldots,L_{\mathrm{f}} \tag{15}$$

a linear system of equations is obtained:

$$A_{k,m,n}q_{k,n} = B_{k,m}, \quad m, n = 1,\ldots,L_{\mathrm{f}} \tag{16}$$

whose coefficients are expressed by dependencies:

$$A_{k,m,n} = \sum_{i=1}^{2}\frac{1}{S_i}\iint_{\mathrm{S}_i}F_{k,m}(\mathbf{r})F_{k,n}(\mathbf{r})\,\mathrm{d}s + d_x^2\sum_{i=3}^{6}\frac{1}{S_i}\iint_{\mathrm{S}_i}G_{k,m}(\mathbf{r})G_{k,n}(\mathbf{r})\,\mathrm{d}s \tag{17}$$

$$B_{k,n} = -U\left(\sum_{i=1}^{2}\frac{1}{S_i}\iint_{\mathrm{S}_i}\varepsilon_{i,k-1}(\mathbf{r})F_{k,n}(\mathbf{r})\,\mathrm{d}s + d_x\sum_{i=3}^{6}\frac{1}{S_i}\iint_{\mathrm{S}_i}\varepsilon_{i,k-1}(\mathbf{r})G_{k,n}(\mathbf{r})\,\mathrm{d}s\right) \tag{18}$$

$$G_{k,n}(\vec{r}) = \frac{\partial F_{k,n}}{\partial n} = \hat{n}\cdot\mathrm{grad}\,F_{k,n}(\mathbf{r}) \tag{19}$$

where $\hat{n}$ is the normal to the surface S_i at $\mathbf{r}$ point.

After numerical solution of the system (16) (e.g. by Gaussian elimination method), the sought set of coefficients $q_{k,n}$ are obtained and the next iteration step follows. In each step, the local error functions (11) - (13) and the boundary error function are calculated, which allows you to control the rate of convergence of the procedure on an ongoing basis and automatically interrupt it when the required accuracy is achieved. Using the basic approximation theorem on the existence and uniqueness of the solution to the linear approximation problem [6], it can be shown that:

$$\delta_k \le \delta_{k-1} \tag{20}$$

which ensures the convergence of the described procedure.

It should be noted that the choice of functions $F_{k,n}$ in (9) boils down to determining their singular points $\mathbf{r}_{k,n}$. As follows from (20), this choice does not affect the exact fact of convergence of the procedure, but the rate of convergence depends on it. There are no general rules on how to make such a choice optimally (in principle, you can create a procedure that would find such an optimal set of points $\mathbf{r}_{k,n}$ in each iteration step, but it is unprofitable from the point of view of the speed of convergence of

the method in real time). In the numerical application created to solve the problem formulated here, in each iterative step, these points are randomly selected from many pregenerated points, uniformly surrounding the Ω area.

The convergence rate of the proposed method also depends on the number of L_f of the fundamental solutions considered in each iteration step. It can be set freely - from $L_f = 1$ to a value limited only by the capacity of the computer's operating memory, which must fit the coefficients of the system of equations (16). The greater the number L_f, the smaller the number of iteration steps needed to obtain the required accuracy and the smaller the total number of fundamental solutions in the final solution (total length of the approximation sum). However, it should be noted that the value of L_f greatly affects the time of a single iteration step, which is mainly influenced by the need to calculate surface integrals occurring in (17) and (18). Numerous numerical experiments by the authors have shown that in many cases the adoption of $L_f = 1$ gives the fastest convergence of the procedure in real time. In this case, the need to numerically solve the system of equations (16) is also avoided.

A certain drawback of the described procedure (e.g. in relation to the classic, collocation version of MRF) is the need to numerically calculate many surface integrals (cf. formulas (14), (17), (18)). This difficulty can be significantly alleviated by using the proper mean square norm, the so-called *pseudonorm*, i.e. assuming the definition of the boundary error functional as:

$$\delta_k = \sqrt{\sum_{i=1}^{6} \frac{1}{L_i} \sum_{j=1}^{L_i} \varepsilon_{i,k}^2 (\mathbf{r}_j)} \tag{21}$$

where $\mathbf{r}_j$ are points distributed densely and more or less evenly on the boundary surfaces of the Ω area. With this approach, formulas (17), (18) take the form:

$$A_{k,m,n} = \sum_{i=1}^{2} \frac{1}{L_i} \sum_{j=1}^{L_i} F_{k,m}(\mathbf{r}_j) F_{k,n}(\mathbf{r}_j) + d_x^2 \sum_{i=3}^{6} \frac{1}{L_i} \sum_{j=1}^{L_i} G_{k,m}(\mathbf{r}_j) G_{k,n}(\mathbf{r}_j) \frac{1}{S_i} \tag{22}$$

$$B_{k,n} = -U\left(\sum_{i=1}^{2} \frac{1}{L_i} \sum_{j=1}^{L_i} \varepsilon_{i,k-1}(\mathbf{r}_j) F_{k,n}(\mathbf{r}_j) + d_x \sum_{i=3}^{6} \frac{1}{L_i} \sum_{j=1}^{L_i} \varepsilon_{i,k-1}(\mathbf{r}_j) G_{k,n}(\mathbf{r}_j) \right). \tag{23}$$

That is, all integrals are replaced by simple sums. The use of a *pseudonorm* instead of a proper norm is formally a less strict approach, because in this case the minimisation of the boundary error applies to a discrete set of boundary points, not to the entire surface. However, it should be noted that any numerical procedure for computing integrals is burdened with a similar inaccuracy because it must also be based on a discrete, "reasonable" representation of the integrand function [7].

2. Simulation results

Using the TSM, the current density distribution in the conductive path of the tested structure was simulated and the examples results are presented in figures 3-4.

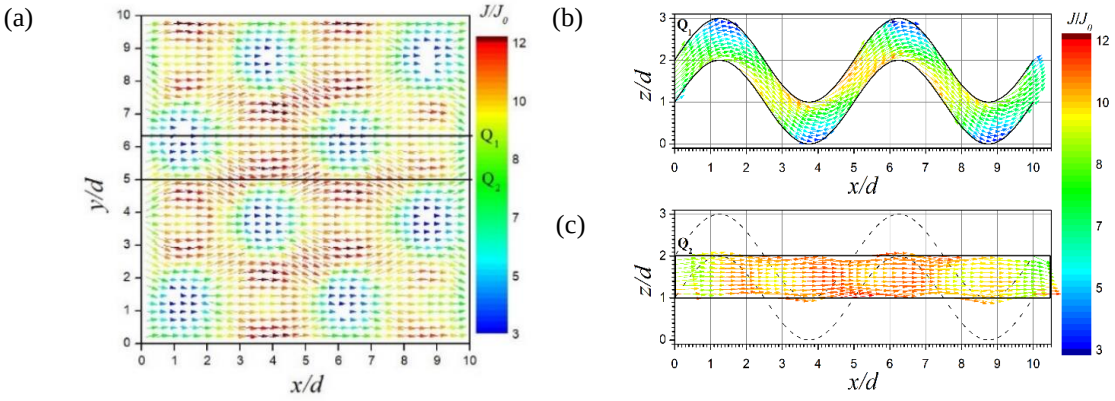

Fig. 3. The current density distribution in the form of a vector field for the 3D TSM illustrated in Fig. 2. Chart (a) illustrates the results in the top surface of the conductive path (S6), however, charts (b) and (c) in the XZ plains for y/d = 6.25 (Q_1) y/d = 5 (Q_2), respectively

Fig. 3 (a) illustrates the current density distribution in the form of a vector field on the top surface of the conductive path (S_6). The lengths of the arrows represent the moduli of the current density vectors calculated as the ratio of the current density J at a given point to the current density J_0 at the same point in the case of a completely flat conductive path. If we compare these results with the graph shown in Fig. 3 (b) which illustrates the same vector field in the XZ plane for $y/d = 6.25$ (see line Q_1 in Fig. 3 (a)), we can see that the current flow is concentrated along the shortest path between the hills of the conductive surface. This nature of the current flow is confirmed by the results in Fig. 3 (c) showing the vector field of the current density in the XZ plane for the parameter $y/d = 5$. This plane does not intersect the hills of the conductive path and is rectangular in shape, which gives an effective cross-section for the current flow and makes the current density the highest here.

The results presented in Fig. 3 allow us to put forward the thesis that roughness on the surface of the conductive path is a significant obstacle to the current flow. To test this thesis, further calculations were carried out, the results of which are shown in Fig. 4.

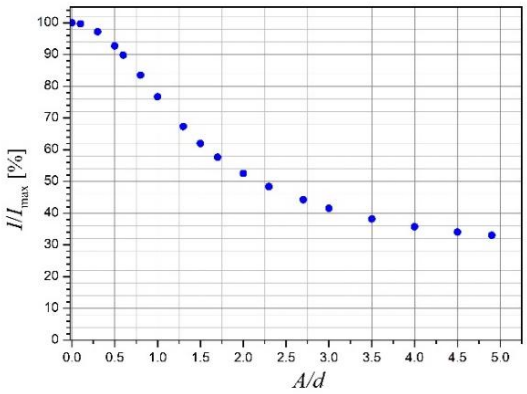

Fig. 4. Changes in the total current (I) of the TSM obtained by increasing the amplitude (A) of the conductive path roughness refer to its maximum value (I_{max}) corresponding to the flat surface of the path.

This figure shows changes in the total current (I) of the TSM obtained by increasing the amplitude ($A = A_1 = A_2$) of the conductive track roughness referring to its maximum value (I_{max}) corresponding to the flat surface of the track. The results confirm the above thesis, as can be seen for a fixed voltage U, as the amplitude of the conductive path roughness increases, the I/I_{max} ratio corresponding to the conductivity of the tested structure decreases. Qualitative confirmation of the above conclusions can be found in the results of measurements carried out in the work [17], where the authors note clear changes in resistivity caused by changes in temperature, which may be due to the smoothing of the conductive surface of the structure.

3. Conclusion

A 3D model of the textronic structure produced by the PVD method was developed. The applied Fundamental Solutions Method ensured accurate and quick calculations of the basic transport parameters of the tested structure. The simulations showed that the current density distribution in a conductive path depends on the nature of its surface, and increasing its roughness reduces its conductance. This gives inspiration for further research focused on the impact of the shape of the conductive path on the properties of ST transport parameters.

Author Contributions: Conceptualization, M.M, S.P., J.P.; methodology, S.P., M.M., J.P; software, S.P., M.M., J.P.; validation, J.P., M.M., S.P.; formal analysis, J.P., S.P., M.M.; investigation, M.M., J.P.; resources, S.P., M.M., J.P.; writing—original draft preparation, M.M. ,S.P.; writing—review and editing, J.P. All authors have read and agreed to the published version of the manuscript.

Literature

[1] Gniotek K., Stempień Z., Zięba J.: Tekstronika - nowy obszar wiedzy (in Polish), Przegląd Włókienniczy + Technik Włókienniczy, 2003, No 2, pp.17-18.
[2] Korzeniewska E., Walczak M., Rymaszewski J.: Elements of elastic electronics created on textile substrate, MIXDES-24thInternational Conference, IEEE, 2017, pp. 447-450.
[3] Jakubas A.: Badania i pomiary wybranych parametrów elektrycznych tekstylnych linii sygnałowych naniesionych metodą maszynową, Przegląd Elektrotechniczny, 2015, Vol. 91, No 12, pp.117-120.
[4] Łada-Tondyra E., Jakubas A.: Nowoczesne zastosowania systemów tekstronicznych (in Polish), Przegląd Elektrotechniczny, 2018, Vol. 94, No 12, pp. 198-201.
[5] Smith, A.A., Li, R. & Tse, Z.T.H. Reshaping healthcare with wearable biosensors. Scientific Reports 13, 4998 (2023). https://doi.org/10.1038/s41598-022-26951-z
[6] Lebioda, M., Rymaszewski, J.: Dynamic properties of cryogenic temperature sensors, Przegląd Elektrotechniczny 2015, 91, 2, 225-227, 10.15199/48.2015.02.51
[7] Tokarska M., Frydrysiak M., Zieba J., Electrical properties of flat textile material as inhomegeneous and anisotropic structure, Journal of Material Science, Materials in Electronics, (2013), 24, 5061–5068
[8] Ates, H.C., Nguyen, P.Q., Gonzalez-Macia, L., Morales-Narváez, E. Güder, F., Collins, J. J., Dincer, C., End-toend design of wearable sensors. Nature Reviews Materials 7, 887–907 (2022), doi.org/10.1038/s41578-022-00460-x
[9] Alonso-González, S. Ver-Hoeye, M. Fernández-García, C. Vázquez-Antuña and F. Las-Heras Andrés, "From Threads to Smart Textile: Parametric Characterization and Electromagnetic Analysis of Woven Structures", IEEE Access, vol. 7, pp. 1486-1501, 2019, doi: 10.1109/ACCESS.2018.2886041
[10] Surname1 N.: Exhaust System for Radial and Axial-Centrifugal Compressor with Pipe Diffuser. International Journal of Turbo and Jet Engines, 2016, Vol. 31, No 1, pp. 29-36.
[11] Dias, T., "Electronic Textiles: Smart Fabrics and Wearable Technology", 1st ed., Woodhead Publishing, Cambridge, UK, 2015)
[12] S. Pawłowski, J. Plewako, E. Korzeniewska, Przegląd Elektrotechniczny 2020, 96, 1 234-237.
[13] S. Pawłowski, J. Plewako, E. Korzeniewska, Electronics 2020, 9, 402.
[14] Kupradze V.D., Aleksidze M.A.: The method of functional equations for the approximate solution of certain boundary value problems (in Russian), USSR Computational Mathematics and Mathematical Physics, Vol. 4, 1964, pp. 82-126.
[15] Achiezer N. I.: Teoria aproksymacji (in Polish), PWN, Warszawa, 1957.
[16] Dryja M., Jankowska J., Jankowski M.: Przegląd metod i algorytmów numerycznych, (in Polish), PWN, Warszawa, 1982.
[17] Lebioda M., Korzeniewska E.: The Influence of Buffer Layer Type on the Electrical Properties of Metallic Layers Deposited on Composite Textile Substrates in the PVD Process. Materials 2023, 16, 4856. https://doi.org/10.3390/ma16134856